Catalysis Today 317 (2018) 108–113

Contents lists available at ScienceDirect

Catalysis Today

journal homepage: www.elsevier.com/locate/cattod

Synthetic natural gas production from CO_2 over Ni-x/CeO_2-ZrO_2 (x = Fe, Co) catalysts: Influence of promoters and space velocity

L. Pastor-Pérez[a,b], E.Le Saché[a], C. Jones[a], S. Gu[a], H. Arellano-Garcia[a], T.R. Reina[a,*]

[a] Department of Chemical and Process Engineering, University of Surrey, Guildford, GU2 7XH, United Kingdom
[b] Laboratorio de Materiales Avanzados, Departamento de Química Inorgánica – Instituto Universitario de Materiales de Alicante Universidad de Alicante, Apartado 99, E-03080 Alicante, Spain

ARTICLE INFO

Keywords:
CO_2 methanation
Ni catalyst
Ceria-zirconia support
Fe and Co promoters
Low-temperature activity

ABSTRACT

Herein, the production of synthetic natural gas is proposed as an effective route for CO_2 conversion. Typical catalysts for this reaction are based on Ni. In this study, we demonstrated that the addition of promoters such as iron and cobalt can greatly benefit the activity of standard Ni methanation catalysts. In particular cobalt seems to be a very efficient promoter. Our Co doped material is an outstanding catalysts for the CO_2 methanation leading to high levels of CO_2 conversion with selectivities close to 100%. Additionally, this catalyst is able to preserve excellent performance at relatively high space velocity which allows flexibility in the reactor design making easier the development of compact CO_2 utilisation units. As an additional advantage, the Co-promoted catalysts is exceptionally stable conserving high levels of CO_2 conversion under continuous operations in long terms runs.

1. Introduction

Climate change and resource depletion are considered two of the greatest and most prominent challenges in modern science. CO_2 is recognised as a major contributor to global climate change, and with the world population continuing to grow and less developed countries becoming increasingly industrialised, solutions are required urgently to tackle this problem. CO_2 utilisation represents a highly attractive solution by converting the emissions into valuable fuels and chemicals, and therefore simultaneously addressing the issue of resource depletion; unlike other carbon-reducing solutions such as carbon capture and storage [1–3]. There are a range of applications when utilising CO_2 as a carbon source [4–7], however this work will discuss the conversion of CO_2 into synthetic natural gas (SNG) via the CO_2 methanation reaction (Eq. (1)).

$$CO_2 + 4H_2 \rightleftarrows CH_4 + 2H_2O,\ \Delta H_{298K} = -165.0\ \text{kJ/mol} \quad (1)$$

Natural gas is considered a clean source of energy compared to burning other fossil fuels due to the reduced emissions of CO_2 [8,9]. For example, it is viewed as one of the cleanest solutions to power the transportation industry and, due to its operational flexibility, can be more easily paired with renewable resources for delivering electricity at peak times. Demand for natural gas has grown over the past few decades [10], and is expected to continue over the coming years.

Several competing reactions, shown in Eqs. (2)–(4), can occur with the reactants and products involved in CO_2 methanation [11] and therefore reduce the selectivity towards methane formation.

$$CO_2 + H_2 \rightleftarrows CO + H_2O,\ \Delta H_{298K} = 41.0\ \text{kJ/mol} \quad (2)$$

$$CO_2 + 2H_2 \rightleftarrows C + 2H_2O,\ \Delta H_{298K} = 90.1\ \text{kJ/mol} \quad (3)$$

$$CO_2 + CH_4 \rightleftarrows 2CO + 2H_2,\ \Delta H_{298K} = 247.3\ \text{kJ/mol} \quad (4)$$

Although CO_2 methanation has the largest equilibrium constant of Eqs. (1)–(4) at lower temperatures, the reverse water-gas shift reaction (Eq. (2)) is typically also present at temperatures above 300 °C. The Bosch reaction (Eq. (3)) and CH_4 reforming reaction (Eq. (4)) only occur at higher temperatures. Therefore, low reaction temperatures thermodynamically favour the targeted reaction (Eq. (1)) over the other potential side reactions [12], but impose kinetic limitations.

CO_2 is a highly stable molecule due to its strong double bonds. Therefore, a catalyst is required to enhance the reaction kinetics, given the low reaction temperature required to favour the reaction thermodynamically. Ni catalysts [12–18] have been the most commonly used in CO_2 methanation due to its combination of high activity and selectivity to CH_4, and relatively low price. Various supports have been used with Ni, including: ZrO_2 [12,18], CeO_2-ZrO_2 [13], Al_2O_3 [14,17], La_2O_3 [16], and CeO_2 [17]. ZrO_2 is interesting for CO_2 methanation due to its acid/base features and CO/CO_2 adsorption capability. Ceria is also used as a support for methanation reaction but combined with ZrO_2 the efficiency of Ni catalysts can be improved. Indeed, ceria introduces

* Corresponding author.
E-mail address: t.ramirezreina@surrey.ac.uk (T.R. Reina).

https://doi.org/10.1016/j.cattod.2017.11.035
Received 11 August 2017; Received in revised form 9 November 2017; Accepted 29 November 2017
Available online 02 December 2017

excellent redox properties to the catalytic formulations due to its high oxygen storage capacity and its population of oxygen vacancies [9]. Therefore, the CeO_2-ZrO_2 support is said to combine the high concentration of oxygen vacancies, high nickel dispersion, and basic properties that CeO_2 and ZrO_2 supports provide individually, whilst also further facilitating the reaction through the particular interaction between the Ni^{2+} cations and ceria-zirconia (CZ) support [15].

Methanation catalysts can include a combination of different active metal phases on one catalyst with the addition of promoters. Synergetic effects of these active metals further promote the adsorption and dissociation of H_2 and CO_2 [19]. Ren et al. [12] demonstrated that the addition of Fe and Co promoters on Ni/ZrO_2 enhanced CO_2 methanation activity, particularly at low temperatures. No investigations have been conducted on ceria-zirconia supported catalysts promoted by other metals despite the promising behaviour of ceria-zirconia as support for this reaction.

On the basis of the above, we have developed a series of Ni supported on CeO_2-ZrO_2 catalysts enhanced with a second metal promoter (Fe or Co) for CO_2 methanation reaction. The influence of the reaction conditions (i.e. the space velocity) as well as the physicochemical properties of the catalysts in the methanation performance are also a subject of this work which aims to provide and strategy to design effective multicomponent catalysts for synthetic natural production from CO_2.

2. Experimental

2.1. Catalyst synthesis

The CeO_2-ZrO_2 support was prepared by the simultaneous co-precipitation method outlined in literature [20]. First, predetermined quantities of nitrates $Ce(NO_3)_3 \cdot 6H_2O$ and $Zr(NO_3)_4 \cdot 6H_2O$ were dissolved in water to give a CeO_2:ZrO_2 ratio of 1.5:1 (all reagents purchased from Sigma-Aldrich). This aqueous solution was co-precipitated with an ammonia solution under vigorous stirring and the pH controlled at around 10 throughout the process. The resulting precipitate was subsequently filtered and washed with distilled water, before drying overnight at 100 °C and calcining in air at 500 °C for 3 h.

Three catalysts were synthesised, with a Ni loading of 15 wt% maintained for all. The first did not contain a promoter, the second 3 wt % Fe, and the third 3 wt% Co; these are respectively denoted NiCZ, NiFeCZ, and NiCoCZ.

The Ni and promoters were loaded onto the CZ supports by co-impregnation method. Nickel nitrate $Ni(NO_3)_2 \cdot 6H_2O$ was used as the nickel precursor, while ferric nitrate $Fe(NO_3)_3 \cdot 9H_2O$ and cobalt nitrate $Co(NO_3)_2 \cdot 6H_2O$ were used as precursors for their respective promoters. First, nickel nitrate was dissolved in water and combined with the requisite amount of CZ support. Promoter nitrate was then added, if necessary, and stirred to form a homogeneous solution, before careful evaporation to dryness under constant stirring at 65 °C. This residue was then dried overnight at 100 °C and calcined in air at 450 °C for 3 h.

2.2. Catalyst characterisation

XRD analysis was conducted on an X'Pert Pro PANalytical diffractometer. Diffraction patterns were recorded using Cu Kα radiation (45 kV, 40 mA) over a 2&z.Theta; range of 10–90°, and a position-sensitive detector using a step size and time of 0.05° and 160 s, respectively. The average crystallite size of the samples were evaluated using the Scherrer equation.

H_2-TPR experiments were carried out in a conventional U-shaped quartz reactor connected to a thermal conductivity detector (TCD). The 5% H_2/Ar reactive gas stream was passed through the catalyst with a total flow of 50 mL min^{-1}. A 10 °C min^{-1} heating rate was utilised to elevate from room temperature to 900 °C. A mixture of ethanol and liquid nitrogen was used as a cold trap to retain the water produced during the reduction.

Textural properties were analysed using nitrogen adsorption-desorption isotherms obtained from a Micromeritics Tristar 22 instrument at −196 °C. Prior to measurement, the samples were degassed for 2 h at 250 °C in vacuum. Specific surface area was calculated by applying the Brunauer-Emmett-Teller (BET) method, and both pore volume and pore size measured using the Barrett-Joyner-Halenda (BJH) method.

Raman spectroscopy measurements were performed on a Thermo Scientific DXR Raman Microscope using a green laser (λ = 532 nm, maximum power 10 mW) with a spot diameter of 0.7 μm and a pinhole aperture of 50 μm. A diffraction grating of 900 grooves mm^{-1}, a CCD detector and a 50× objective were used.

2.3. CO_2 methanation activity

CO_2 methanation was performed in a continuous fixed bed quartz reactor using 250 mg of catalyst in each test. Prior to the reaction, the catalysts were reduced in situ in a 20% H_2/N_2 stream for 2 h with a total gas flow of 200 mL min^{-1} at 400 °C. The flow of reactants was held at a constant weight hourly space velocity (WHSV) of 12,500 mL g^{-1} h^{-1} with a H_2/CO_2 ratio of 4:1 balanced in nitrogen. The reaction temperature was varied between 200 and 400 °C, with 50 °C intervals. Reactants and products were monitored by online gas analyser (ABB AO2020) equipped with IR and TCD detectors. The effluent compositions were recorded once the reaction had reached steady-state at each temperature interval.

For the analysis of the effect of space velocity on catalyst performance, the reaction conditions were tested at the same temperatures and H_2/CO_2 ratio at space velocities of 6250, 12,500 and 25,000 mL g^{-1} h^{-1}. The stability test was conducted for 50 h at 300 °C and a space velocity of 14,000 mL g^{-1} h^{-1}.The CO_2 conversion and CH_4 selectivity are defined according to Eqs. (5) and (6) [21]:

$$X_{CO_2}(\%) = \frac{[CO_2]_{in} - [CO_2]_{out}}{[CO_2]_{in}} \text{x100} \quad (5)$$

$$S_{CH_4}(\%) = \frac{[CH_4]_{out}}{[CO_2]_{in} - [CO_2]_{out}} \text{x100} \quad (6)$$

where $[CO_2]_{in}$ and $[CO_2]_{out}$ are CO_2 inlet and outlet mole concentrations, respectively and $[CH_4]_{out}$ is the methane outlet mole concentration.

3. Results and discussion

3.1. Catalyst characterisation results

Fig. 1 displays the XRD patterns of the calcined samples. The XRD pattern of the bare CZ support is also shown for comparison. The characteristic peaks of NiO fcc phase at 2θ = 37°, 43° and 63° can be

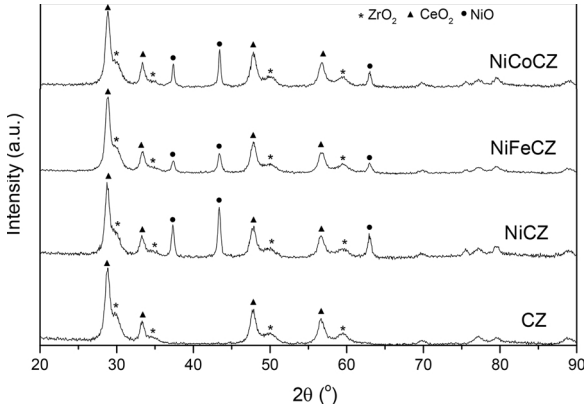

Fig. 1. XRD patterns of the calcined CZ support and the calcined catalysts.

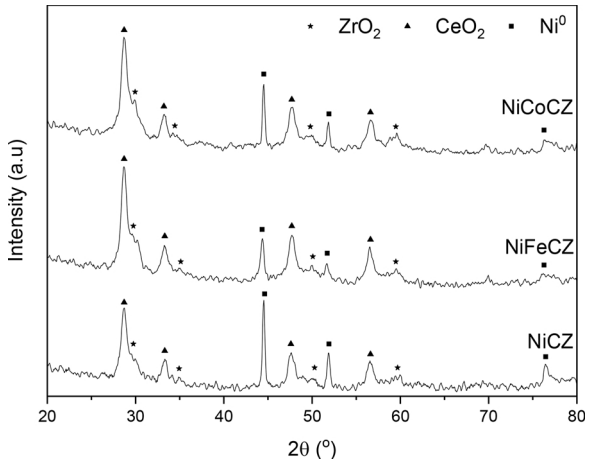

Fig. 2. XRD patterns of the reduced catalysts.

seen in all samples [22]. The non-promoted NiCZ catalyst presented the most intense peak with a particle size around 17 nm. Nevertheless, the presence of Fe and Co enhanced the tolerance towards sintering in the Ni-based catalysts obtaining Ni particles of around 6 and 11 nm respectively in good agreement with previous studies in literature [23].

Peaks at 2θ values of 29.4°, 34.0°, 48.8° and 58.0° are said to correspond to the presence of a single fluorite-shape $Ce_xZr_{1-x}O_2$ phase [13]. However, Fig. 1 suggests the segregation of the CeO_2 and ZrO_2 into individual oxide phases due to the presence of shoulders on each of these peaks. According to literature [24], signals for CeO_2 and ZrO_2 arise at 2θ values of 28.6°, 33.5°, 48.0°, and 57.0°, and 30.2°, 35.2°, 50.5°, and 60°, respectively. The peaks (CeO_2) and shoulders (ZrO_2) shown in Fig. 1 more closely align with these 2θ values than those of $Ce_xZr_{1-x}O_2$. Characteristic peaks for the Fe (FeO_x) and Co (CoO_x) promoters do not appear in XRD profiles of the fresh materials due to a combination of factors: their quantity being too small and their particles well-dispersed over the $Ce_xZr_{1-x}O_2$ support.

Additional information is extracted from the X-Ray diffraction patterns of the reduced samples in Fig. 2. Indeed, the activation step performed before each catalytic run has the objective to reduce the metal oxides to active metallic particles. Fig. 2 reveals the complete reduction of NiO species present in the calcined catalysts to metallic Ni^0 particles (JCPDS# 45–1027). Once again, no peaks characteristic of Fe or Co are detected.

Redox properties are relevant in hydrogenation reactions such as the CO_2 methanation. In this sense, the reducibility of the catalysts were investigated by H_2-TPR, the profiles of which are shown in Fig. 3. Each profile has a major peak located between 300 and 380 °C. According to literature, these peaks are due to the reduction of Ni^{2+} to Ni^0 species [25,26]. A small shoulder is present on the major peak of the NiCZ catalyst at approximately 340 °C which can be attributed to the surface reduction of reducible CeO_2 species in close contact to Ni in the CZ support [13]. The NiFeCZ and NiCoCZ samples present higher homogeneous reduction peak area that can be due to the joint reduction of Ni-Ce-promoter species.

Table 1
Textural properties of the CZ support and all catalysts.

Catalyst	Surface area[a] (m^2/g)	Pore Volume[b] (cm^3/g)	Pore Size[c] (nm)
CZ	40	0.06	4.75
NiCZ	36	0.11	9.11
NiFeCZ	37	0.09	7.32
NiCoCZ	29	0.05	5.42

[a] Calculated by the BET equation.
[b] BJH desorption pore volume.
[c] BJH desorption average pore diameter.

The textural properties of the Ni-based catalysts and the support derived from N_2 physisorption are listed in Table 1 and the obtained isotherms are shown in Fig. 4. According to the IUPAC standards, the obtained nitrogen isotherms can be classified as type IV, characteristic of mesoporous materials [26,27]. The addition of Ni and the promoters is shown to slightly reduce the surface area of the bare CZ support. In any case, the pore size distributions were within the mesoporous range for all catalysts, and there was little difference between in terms of textural properties among the studied materials.

3.2. CO_2 methanation activity results

3.2.1. Effect of promoter on catalytic performance

Fig. 5 shows CO_2 conversion for the three catalysts. At the low temperature range (i.e. 200 °C) relatively poor catalytic activity was observed with the Fe doped catalysts, even though duplicating the activity obtained with NiCZ and NiCoCZ. However an increase in reaction temperature caused an increase in CO_2 conversion until 400 °C; with the sharpest increase occurring between 250 and 300 °C. CO_2 conversions of 71, 58 and 83% were achieved at 300 °C for the NiCZ, NiFeCZ and NiCoCZ catalysts, respectively. Interestingly, although the Fe promoted catalyst achieved the greatest CO_2 conversion at low temperatures its performance is relatively poor in the medium and high temperature range compare to that of the other two catalysts. As reported by Ren et al. [12] with the addition of Fe, most of the CO_2 dissociates into CO rather than forming hydrogen carbonates, monodentate carbonates, and bicarbonate species, and the CO_2 adsorption capacity of the catalyst increases at lower temperatures. NiCoCZ and NiCZ

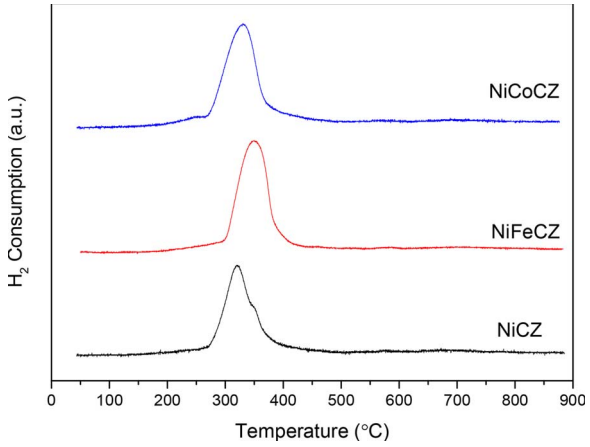

Fig. 3. H_2-TPR profiles for all catalysts.

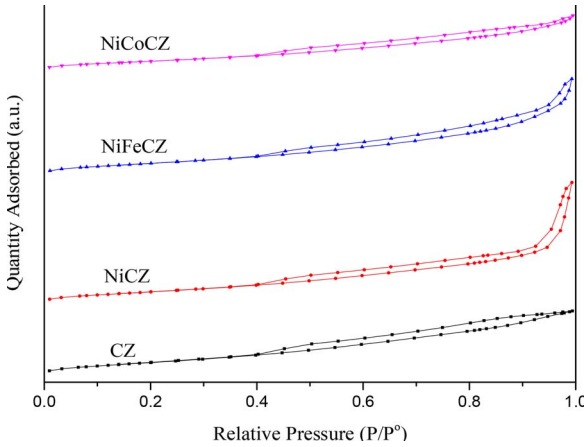

Fig. 4. N_2 adsorption-desorption isotherms of the CZ support and all catalysts.

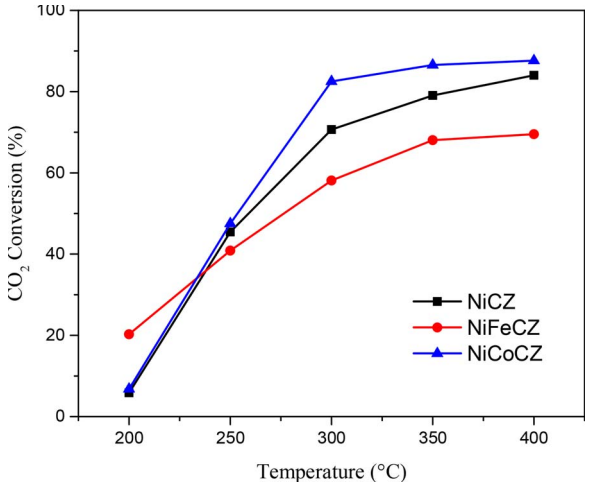

Fig. 5. CO_2 conversion for Ni/CZ, NiFe/CZ and NiCo/CZ catalysts.

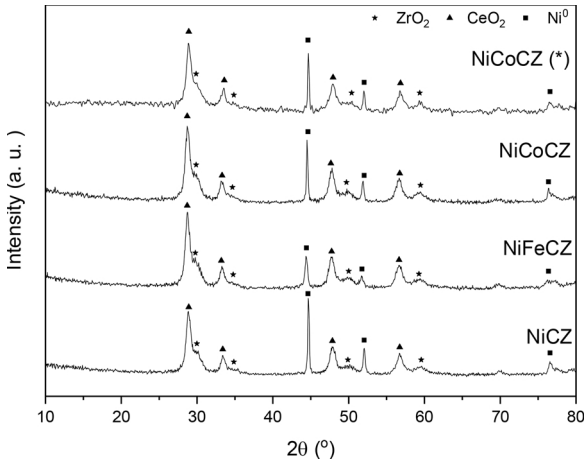

Fig. 7. XRD patterns of the catalysts after the reaction; (*) after the 50 h stability test.

performed similarly below 250 °C, but notorious improvement is shown by the Co promoted catalyst at higher temperatures. It is well reported that Co catalysts have the advantage of decrease coke deposition due to its excellent redox properties ($Co_3O_4 \rightarrow CoO \rightarrow Co^{\circ}$) [28,29]. In this sense more active sites are available, a fact that mostly agrees with the high CO_2 conversion achieved by this catalysts in comparison with the non-promoted Ni catalyst. In addition, we have selected CZ support due the exceptional redox properties of both Ce and Zr that make them excellent carriers for this reaction. Indeed, this type of supports outstands for its high concentration of oxygen vacancies on the catalysts surface, which are of key importance for the dissociative adsorption of CO_2, and also have a very important role in gasifying carbon deposits compared with other supports [13,15].

Fig. 6 displays selectivity towards CH_4 for the catalysts over the different reaction temperatures studied. CH_4 selectivity across all three catalysts was lowest at the temperature extremes and highest in the middle around approximately 300 °C, in good agreement with the reaction thermodynamics. This is similar to most other trends in literature, where the selectivity initially increases before the reverse water-gas shift reaction takes place above 350 °C and starts to produce CO [13]. CH_4 selectivities of 78, 73 and 93% were achieved at 300 °C for the NiCZ, NiFeCZ and NiCoCZ catalysts, respectively. The Ni-CoCZ catalyst shows the highest level of CH_4 selectivity above 205 °C and maintains it across the studied temperature range in agreement with the explained before. Therefore, considering both the CO_2 conversion and CH_4 selectivity the catalysts can be ranked as follows: NiCoCZ > NiCZ > NiFeCZ. Accordingly, the NiCoCZ catalyst was selected for further experiments due to its better activity/selectivity balance and also the fact that Co-doped NiCZ materials are under explored for the methanation process.

Fig. 7 shows the XRD patterns of the spent NiCZ, NiFeCZ and Ni-CoCZ catalysts. The post reaction XRD analysis reveals that Ni remains as metallic after the reaction. Furthermore, Ni sintering is more notorious for non-promoted catalyst (26 nm) and a moderate increase in the Ni particle size was detected for the NiFeCZ (11 nm) and NiCoCZ (19 nm) samples after the reaction. The later exhibits the role of promoters: they not only promote the catalytic activity but also improve Ni dispersion and stability during the methanation reaction.

3.2.2. *Effect of space velocity on catalytic performance*

Reactor manufacturing in general and reactor volume in particular is one of the main contribution to the capital cost expenditure for any potential application of CO_2 utilisation units. In this sense, it is interesting to study the effect of the space velocity in the catalytic behaviour of the developed catalysts. For this study the best performing catalyst NiCoCZ was selected. These experiments were carried out using the same reaction conditions except the space velocity was changed to 6250 and 25,000 mL g^{-1} h^{-1}. Fig. 8 shows the CO_2 conversion versus reaction temperature for the three different space velocities investigated; an overall trend of slightly increasing CO_2 conversion can be seen when space velocity is reduced. On the other hand, an increase in space velocity (25,000 mL g^{-1} h^{-1}) caused a more notorious decreased in the catalytic activity, still being a good CO_2 conversion level, reaching 60%

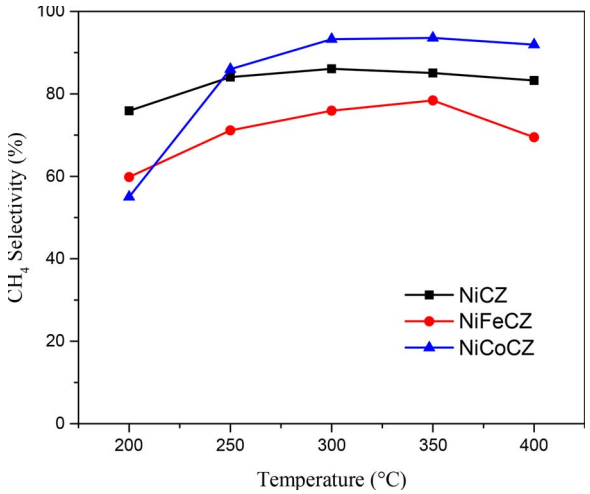

Fig. 6. CH_4 selectivity for Ni/CZ, NiFe/CZ and NiCo/CZ catalysts.

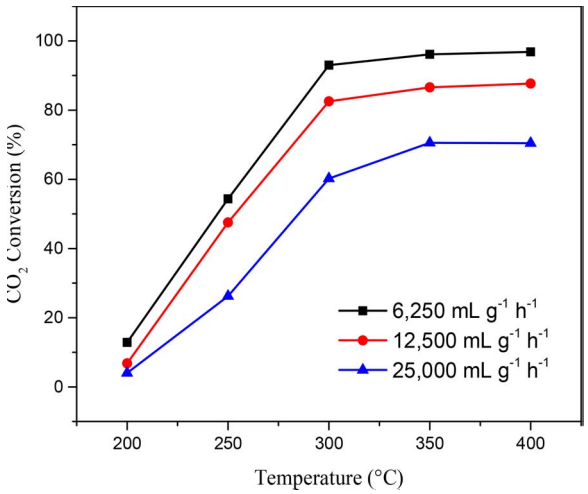

Fig. 8. CO_2 conversion for Ni-Co/CZ catalyst at different space velocities.

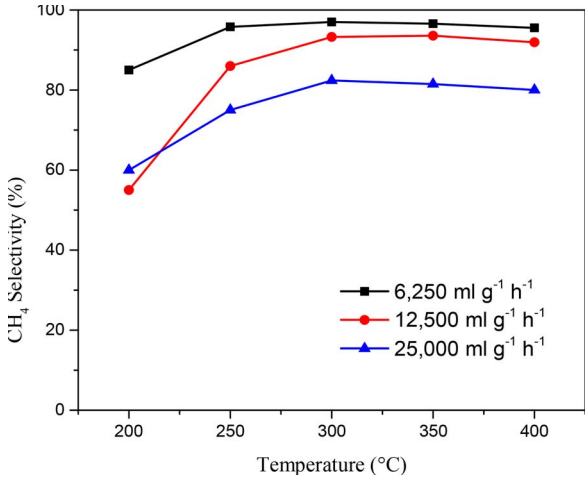

Fig. 9. CH_4 selectivity for Ni-Co/CZ catalyst at different space velocities.

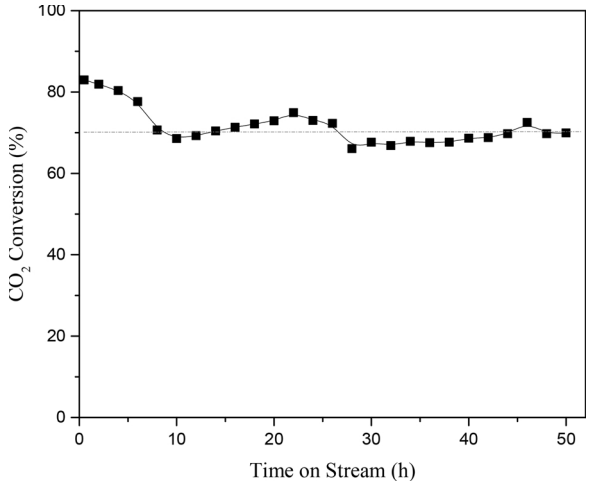

Fig. 10. Stability test for NiCoCZ catalyst at 300 °C and 14,000 mL g^{-1} h^{-1}.

at 300 °C. This results indicate that our catalysts could achieve good levels of synthetic natural gas production with relatively small reactor volumes (large space velocities) what helps to intensify the process.

Fig. 9 shows CH_4 selectivity for the different space velocities studied. Once again, the reduced space velocity appears to enhance the catalytic activity as the 6250 mL g^{-1} h^{-1} sample achieves selectivities consistently around 98% from 250 to 400 °C. In contrast, for the sample at 25,000 mL g^{-1} h^{-1} CH_4 selectivity reaches a maximum of 82% at 300 °C which is still a good result considering the demanding reaction conditions.

In order to establish a more general comparison with previously reported Ni-Ce-Zr methanation catalysts, different reported catalysts and the conditions used in the CO_2 methanation are presented in Table 2. As shown in the table, our NiCoCZ catalyst can be deemed to perform a superior behaviour in the compared conditions. Furthermore, our catalysts continues showing a good performance tested at higher space velocities, what reinforces the exceptional behaviour of the developed system. The balance between the low Ni loading, high CO_2 conversion-CH_4 selectivity and the relatively high space velocity used, highlights the excellent results of our catalyst in the CO_2 methanation reaction.

3.2.3. Stability test

Finally, the catalysts stability for long term operations was tested since this is a fundamental pre-requisite for a potential application. Fig. 10 shows the CO_2 conversion during 50 h on stream at 300 °C for the NiCoCZ catalyst. The initial level of conversion was 83%, which decreased to 70% after 8 h of activity. After the slight activity drop the conversion remained stable around 70% for the following 42 h. As for the CH_4 selectivity, this was rather high throughout the entire run, consistently remaining above 90%.

The promising performance of the Co-doped catalyst in terms of stability is partially due to its robustness to sintering and carbon deposition resistance as previously revealed by the XRD of the post reaction sample in Fig. 7. In addition to the limited sintering of Ni, no peaks related to carbon were found on the post reaction profile of NiCoCZ after 50 h of continuous reaction revealing the great resistance of our catalysts to carbon formation even for long runs. This claim is supported by TGA analysis performed in air on samples after reaction (not shown for briefness) where no weight loss other than water evaporation was observed. No signs of carbon deposition (or at least hard crystalline carbon deposits) have been detected, a fact corroborated by Raman spectroscopy of the NiCoCZ catalyst having underwent 50 h of reaction (Fig. 11).

The spectrum shows one strong Raman peak at 477 cm^{-1} (F_{2g} mode of cubic CeO_2) and a weak band at 490 cm^{-1}, attributed to the presence of defective structure (electron defect or O-vacancy) in the CeO_2–ZrO_2 mixed oxide [31]. Also, weaker bands between 310 and 370 cm^{-1}, originating from the six Raman active modes ($A_{1g} + 2B_{1g} + 3E_g$) of tetragonal ZrO_2 [32], can be observed along with a second order Raman peak prominent at 1088 cm^{-1}. As mentioned aboved, Raman peaks related to carbon, typically the D band at 1350 cm^{-1} and the G band at 1585 cm^{-1} are not present confirming the absence of notable carbon deposition on the catalyst's surface.

Table 2
Catalysts employed and conditions used in catalytic CO_2 methanation. .

Catalyst	CO_2 Conv. (%)	CH_4 sel. (%)	Temp (°C)	Pressure (bar)	H_2/CO_2	Space Velocity
10Ni-CeO_2 [17]	90	100[a]	300	1.01	4:1	10,000 h^{-1} (300 mg)
5Ni-CZ [15]	63	–	300	1.01	4:1	22,000 mL g^{-1} h^{-1}
5Ni-0.5Ru-CZ [15]	55	–	300	1.01	4:1	22,000 mL g^{-1} h^{-1}
10Ni-CZ [13]	55	97	300	1.01	4:1	20,000 mL g^{-1} h^{-1}
20Ni-2Ce-Al_2O_3 [30]	78	100[b]	300	1.01	3.5:1	9000 mL g^{-1} h^{-1}
10Ni-La_2O_3 [16]	90	100[a]	300	1.5	4:1	3250 h^{-1} (1 g)
30Ni-3Co- ZrO_2 [12]	100	94	300	5	4:1	4980 mL g^{-1} h^{-1}
30Ni-3Fe-ZrO2 [12]	100	94	300	5	4:1	4980 mL g^{-1} h^{-1}
15Ni-ZrO_2 [28]	60	100	300	10	4:1	48,000 mL g^{-1} h^{-1}
30Ni-5Fe-Al_2O_3 [14]	58.5	58	220	10	4:1	9600 mL g^{-1} h^{-1}
NiCZ	71	86	300	1.01	4:1	12,500 mL g^{-1} h^{-1}
NiFeCZ	58	76	300	1.01	4:1	12,500 mL g^{-1} h^{-1}
NiCoCZ	83	94	300	1.01	4:1	12,500 mL g^{-1} h^{-1}
NiCoCZ	60	82	300	1.01	4:1	25,000 mL g^{-1} h^{-1}

[a] No specified.

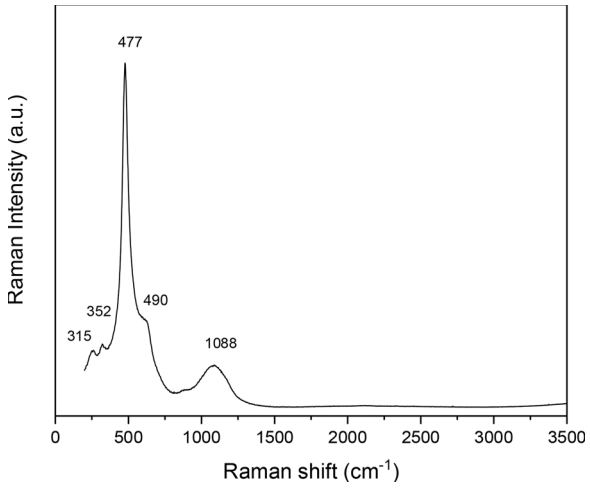

Fig. 11. Raman spectra of NiCoCZ after 50 h of stability test.

In this scenario, it can be concluded that our cobalt-doped Ni-ceria/zirconia is an excellent catalysts for the production of synthetic methane from CO_2, exhibiting a great compromise activity/selectivity and outstanding stability for long runs reactions plus superior behaviour than similar catalysts reported in the literature.

4. Conclusions

A series of highly efficient catalysts for synthetic natural gas production from CO_2 has been developed in this work. These materials are based on Ni particles supported on ceria-zirconia. Our findings reveal that the use of promoters such as FeOx and CoOx boosts the catalytic performance of a reference NiCZ sample. However, the degree of activity promotion depends on the type of dopant. Fe only improves the activity in the low temperature range while Co greatly benefits the CO_2 conversion at medium-high temperatures. Overall, the Co based catalysts is the most efficient material within the studied series showing not only an excellent activity/selectivity balance but also exceptional stability for long term runs. Furthermore, this catalysts is able to maintain high levels of activity and selectivity at relatively high space velocity which in turns may impact the reactor design facilitating compact reactor configurations. Therefore, the multicomponent NiCoCZ catalyst is proposed as a novel promising catalyst for CO_2 utilization via methanation processes.

Acknowledgment

The authors of this work would like to acknowledge the Department of Chemical and Process Engineering at the University of Surrey for the access to technical equipment. Also financial support for this work has been obtained from the EPSRC grants no EP/J020184/2 and EP/R512904/1. L. Pastor-Perez acknowledges Generalitat Valenciana for her postdoctoral grant (APOSTD/2017).

References

[1] K. van Alphen, J. van Ruijven, S. Kasa, M. Hekkert, W. Turkenburg, Energy Pol. 37 (2009) 43–55.
[2] Y. Wu, C. Chan, Expert Syst. Appl. 36 (2009) 9949–9960.
[3] E. Mechleri, A. Lawal, A. Ramos, J. Davison, N.M. Dowell, Int. J. Greenhouse Gas Conserv. 57 (2017) 14–25.
[4] C.R. Jones, R.L. Radford, K. Armstrong, P. Styring, J. CO_2 Util. 7 (2014) 51–54.
[5] B. Yao, W. Ma, S. Gonzalez-Cortes, T. Xiao, P.P. Edwards, Greenhouse Gas Sci. Technol. 0 (2017) 1–15.
[6] X. Du, B. Yao, S. Gonzalez-Cortes, V.L. Kuznetsov, H. AlMegren, T. Xiao, P.P. Edwards, Faraday Discuss. 183 (2015) 161–176.
[7] A. Alvarez, A. Bansode, A. Urakawa, A.V. Bavykina, T.A. Wezendonk, M. Makkee, J. Gascon, F. Kapteijn, Chem. Rev. 117 (2017) 9804–9838.
[8] J. Speight, Hydrocarbon Process. 88 (2009) 67–70.
[9] J.J. Spivey, G. Hutchings, Chem. Soc. Rev. 43 (2014) 792–803.
[10] R. Burch, N. Parkyns, Chem. Br. 28 (1992) 1013.
[11] J. Gao, Y. Wang, Y. Ping, D. Hu, G. Xu, F. Gu, F. Su, RSC Adv. 2 (2012) 2358–2368.
[12] J. Ren, X. Qin, J.-Z. Yang, Z.-F. Qin, H.-L. Guo, J.-Y. Lin, Z. Li, Fuel Process. Technol. 137 (2015) 204–211.
[13] J. Ashok, M.L. Ang, S. Kawi, Catal. Today 281 (2017) 304–311.
[14] S. Hwang, U.G. Hong, J. Lee, J.G. Seo, J.H. Baik, D.J. Koh, H. Lim, I.K. Song, J. Ind. Eng. Chem. 19 (2013) 2016–2021.
[15] F. Ocampo, B. Louis, L. Kiwi-Minsker, A.-C. Roger, Appl. Catal. A: Gen. 392 (2011) 36–44.
[16] H. Song, J. Yang, J. Zhao, L. Chou, Chin. J. Catal. 31 (2010) 21–23.
[17] S. Tada, T. Shimizu, H. Kameyama, T. Haneda, R. Kikuchi, Int. J. Hydrogen Energy 37 (2012) 5527–5531.
[18] K. Zhao, W. Wang, Z. Li, J. CO_2 Util. 16 (2016) 236–244.
[19] M. Younas, L. Kong, M. Bashir, H. Nadeem, A. Shehzad, S. Sethupathi, Energy Fuels 30 (2016) 8815–8831.
[20] L. Lan, S. Chen, Y. Cao, M. Zhao, M. Gong, Y. Chen, J. Colloid Interface Sci. 450 (2015) 404–416.
[21] J.K. Kirchner, H. Lösch, S. Kureti, Appl. Catal. B: Env (2017), http://dx.doi.org/10.1016/j.apcatb.2017.06.025 (in press).
[22] L. Pastor- Pérez, A. Sepúlveda-Escribano, Appl. Catal. A: Gen. 529 (2017) 118–126.
[23] H. Lu, X. Yang, G. Gao, J. Wang, C. Han, X. Liang, C. Li, Y. Li, W. Zhang, X. Chen, Fuel 183 (2016) 335–344.
[24] M. Alifanti, B. Baps, N. Blangenois, J. Naud, P. Grange, B. Delmon, Chem. Mater 15 (2003) 395–403.
[25] M. Ang, U. Oemar, E.T. Saw, L. Mo, Y. Kathiraser, B.H. Chia, S. Kawi, ACS Catal. 4 (2014) 3237–3248.
[26] Z.A. ALOthman, Materials 5 (2012) 2874–2902.
[27] C. Wang, N. Sun, M. Kang, X. Wen, N. Zhao, F. Xiao, W. Wei, T. Zhao, Y. Sun, Catal. Sci. Technol. 3 (2013) 2435–2443.
[28] Y.Y. Itkulova, S.K. Nurmakanov, Catal. Today (2017), http://dx.doi.org/10.1016/j.cattod.2017.07.014 (in press).
[29] Zs. Ferencz, K. Baán, A. Oszkó, Z. Kónya, T. Kecskés, A. Erdőhelyi, Catal. Today 228 (2014) 123–130.
[30] S. Rahmani, M. Rezaei, F. Meshkani, J. Ind. Eng. Chem. 20 (2014) 4176–4182.
[31] J.R. Kim, W.J. Myong, S.K. Ihm, J. Catal. 263 (2009) 123–133.
[32] W. Mista, T. Rayment, J. Hanuza, L. Macalik, Mater. Sci. Poland 22 (2004) 153–170.